

## Electronic Supplementary Information

### **AuB<sub>8</sub><sup>-</sup>: An Au-Borozone Complex**

Wei-Jia Chen<sup>1,4</sup>, Yang-Yang Zhang<sup>2,4</sup>, Wan-Lu Li<sup>2</sup>, Hyun Wook Choi<sup>1</sup>, Jun Li<sup>2,3\*</sup> and Lai-Sheng Wang<sup>1\*</sup>

<sup>1</sup>Department of Chemistry, Brown University, Providence, RI 02912, United States.

<sup>2</sup>Department of Chemistry and Key Laboratory of Organic Optoelectronics & Molecular Engineering of Ministry of Education, Tsinghua University, Beijing 100084, China.

<sup>3</sup>Department of Chemistry, Southern University of Science and Technology, Shenzhen 518055, China.

<sup>4</sup>These authors contributed equally: Wei-Jia Chen, Yang-Yang Zhang.

\*Email: [junli@tsinghua.edu.cn](mailto:junli@tsinghua.edu.cn); [lai-sheng\\_wang@brown.edu](mailto:lai-sheng_wang@brown.edu)

## Experimental and theoretical methods

### Photoelectron spectroscopy

The experiment was carried out with a magnetic-bottle PES apparatus equipped with a laser vaporization cluster source. More details can be found in previous publications.<sup>1,2</sup> In this study, the  $\text{AuB}_8^-$  cluster was produced by laser ablation of a  $\text{Au}^{10}\text{B}$  target, prepared by mixing powders of Au and 97%-enriched  $^{10}\text{B}$  in a glove box. The laser-induced plasma was quenched by a helium carrier gas seeded with 5% argon to initiate nucleation and cluster growth. Clusters formed in the nozzle were entrained by the carrier gas and underwent a supersonic expansion. After passing through a skimmer, anionic clusters in the collimated molecular beam were extracted perpendicularly into a time-of-flight mass spectrometer. The  $\text{AuB}_8^-$  cluster was mass-selected and decelerated before being photodetached by the 193 nm photons (6.424 eV) from an ArF excimer laser, or the 355 nm (3.496 eV) and 266 nm (4.661 eV) photons from a Nd:YAG laser. Photoelectrons were collected with >90% efficiency by the magnetic-bottle and analyzed in a 3.5 m long time-of-flight tube. The photoelectron kinetic energies were calibrated using the known atomic transitions of  $\text{Bi}^-$ . The kinetic energy ( $E_k$ ) resolution ( $\Delta E_k/E_k$ ) of the magnetic-bottle apparatus was about 2.5%, that is,  $\sim 25$  meV for 1eV electrons.

### Computational methods

The global minimum (GM) structures of  $\text{AuB}_8^{0/-}$  were searched using the Tsinghua Global Minimum (TGMin)<sup>3,4</sup> software, which was based on the Basin-Hopping algorithm.<sup>5</sup> More than 1200 local minimum structures for  $\text{AuB}_8^{0/-}$  with various spin multiplicities were examined using the Gaussian 16 package.<sup>6</sup> Density functional theory (DFT) at the hybrid B3LYP level<sup>6,7</sup> was used initially with the 6-311+G(d) basis set<sup>8</sup> for B, and the Lanl2DZ basis set<sup>9</sup> and the corresponding pseudopotential for Au. All local minima (LMs) were verified through calculations of the harmonic vibrational frequencies. Subsequently, low-lying isomers within a B3LYP energy range of 100 kcal/mol were re-optimized using the Perdew-Burke-Ernzerhof (PBE) functional<sup>10</sup> and the hybrid PBE0 exchange-correlation functional<sup>11</sup>. These calculations used Slater-type basis sets with the triple- $\zeta$  plus one polarization function (TZP)<sup>12</sup> in the ADF 2021.101 package.<sup>13</sup> The scalar relativistic (SR) effects were taken into account in the calculations with the zero-order regular approximation (ZORA).<sup>14</sup> The frozen-core approximation was applied to the  $[1s^2]$  core of B and the  $[1s^2-4d^{10}]$  core of Au. In order to obtain more accurate relative energies, we further performed single-point *ab initio* DLPNO-CCSD(T) calculations for the three lowest-lying isomers using the ORCA 4.2.0 package<sup>15</sup> with the structures optimized at the PBE0/TZP level. The DLPNO-CCSD(T) calculations were done using the all-electron Def2-TZVP basis set for both B and Au.

The first adiabatic detachment energy (ADE) and the first vertical detachment energy (VDE) were calculated both at the PBE and PBE0 levels. In order to compare with the experimental PES data, we calculated higher VDEs approximately using the  $\Delta\text{SCF-TDDFT}$  method<sup>16</sup> combined with the SAOP exchange-correlation functional.<sup>17</sup> Chemical bonding was analyzed using the canonical Kohn-Sham molecular orbitals (MOs), as well as the adaptive natural density partitioning (AdNDP) approach<sup>18</sup> at the B3LYP/LANL2DZ/6-311G\* level. The atomic charges with the formalisms of Mulliken charge populations,<sup>19</sup> Hirshfeld,<sup>20</sup> Voronoi<sup>21</sup> and multipole-derived charge (MDC)<sup>22</sup> and NPA were also calculated at the PBE/TZP level with the SR-ZORA effect.

## References:

- 1 L. S. Wang, *Int. Rev. Phys. Chem.*, 2016, **35**, 69-142.
- 2 L. S. Wang, H. S. Cheng and J. Fan, *J. Chem. Phys.*, 1995, **102**, 9480–9493.
- 3 Y. F. Zhao, X. Chen and J. Li, *Nano Res.*, 2017, **10**, 3407-3420.
- 4 X. Chen, Y. F. Zhao, Y. Y. Zhang and J. Li, *J. Comput. Chem.*, 2019, **40**, 1105-1112.
- 5 D. J. Wales and J. P. Doye, *J. Phys. Chem. A*, 1997, **101**, 5111-5116.
- 6 M. J. Frisch, G. W. Trucks, H. B. Schlegel, G. E. Scuseria, M. A. Robb, J. R. Cheeseman, G. Scalmani, V. Barone, G. A. Petersson, H. Nakatsuji, X. Li, M. Caricato, A. V. Marenich, J. Bloino, B. G. Janesko, R. Gomperts, B. Mennucci, H. P. Hratchian, J. V. Ortiz, A. F. Izmaylov, J. L. Sonnenberg, D. Williams-Young, F. Ding, F. Lipparini, F. Egidi, J. Goings, B. Peng, A. Petrone, T. Henderson, D. Ranasinghe, V. G. Zakrzewski, J. Gao, N. Rega, G. Zheng, W. Liang, M. Hada, M. Ehara, K. Toyota, R. Fukuda, J. Hasegawa, M. Ishida, T. Nakajima, Y. Honda, O. Kitao, H. Nakai, T. Vreven, K. Throssell, J. A. Montgomery, Jr., J. E. Peralta, F. Ogliaro, M. J. Bearpark, J. J. Heyd, E. N. Brothers, K. N. Kudin, V. N. Staroverov, T. A. Keith, R. Kobayashi, J. Normand, K. Raghavachari, A. P. Rendell, J. C. Burant, S. S. Iyengar, J. Tomasi, M. Cossi, J. M. Millam, M. Klene, C. Adamo, R. Cammi, J. W. Ochterski, R. L. Martin, K. Morokuma, O. Farkas, J. B. Foresman, and D. J. Fox, Gaussian 16, Revision A.03, Gaussian, Inc., Wallingford CT, 2016.
- 6 W. Kohn and L. J. Sham, *Phys. Rev.*, 1965, **140**, 1133-1138.
- 7 A. D. Becke, *J. Chem. Phys.*, 1993, **98**, 5648-5652.
- 8 B. P. Pritchard, D. Altarawy, B. T. Didier, T. D. Gibson and T. L. Windus. *J. Chem. Inf. Model.*, 2019, **59**, 4814-4820.
- 9 B. T. Didier, T. Elsethagen, L. Sun, V. Gurumoorthi, J. Chase, J. Li and T. L. Windus, *J. Chem. Inf. Model.*, 2007, **47**, 1045-1052.
- 10 J. P. Perdew, K. Burke and M. Ernzerhof, *Phys. Rev. Lett.*, 1996, **77**, 3865-3868.
- 11 C. Adamo and V. Barone, *J. Chem. Phys.*, 1999, **110**, 6158-6170.
- 12 E. v. Lenthe and E. J. Baerends, *J. Comput. Chem.*, 2003, **24**, 1142-1156.
- 13 ADF, SCM, Theoretical Chemistry, Vrije Universiteit, Amsterdam, The Netherlands, <http://www.scm.com>.
- 14 E. v. Lenthe, E. J. Baerends and J. G. Snijders, *J. Chem. Phys.*, 1993, **99**, 4597-4610.
- 15 F. Neese, The ORCA program system. *Wiley Interdiscip. Rev. Comput. Mol. Sci.*, 2012, **2**, 73-78.
- 16 J. Li, X. Li, H. J. Zhai and L. S. Wang, *Science*, 2003, **299**, 864-867.
- 17 P. Schipper, O. Gritsenko, S. v. Gisbergen and E. J. Baerends, *J. Chem. Phys.*, 2000, **112**, 1344-1352.
- 18 D. Y. Zubarev and A. I. Boldyrev, *Phys. Chem. Chem. Phys.*, 2008, **10**, 5207-5217.
- 19 R. S. Mulliken, *J. Chem. Phys.*, 1955, **23**, 1833-1840.
- 20 F. L. Hirshfeld, *Theor. Chim. Acta*, 1977, **44**, 129-138.
- 21 F. M. Bickelhaupt, N. J. v. E. Hommes, C. F. Guerra and E. J. Baerends, *Organometallics*, 1996, **15**, 2923-2931.
- 22 M. Swart, P. T. van Duijnen and J. G. Snijders, *J. Comput. Chem.*, 2001, **22**, 79-88.

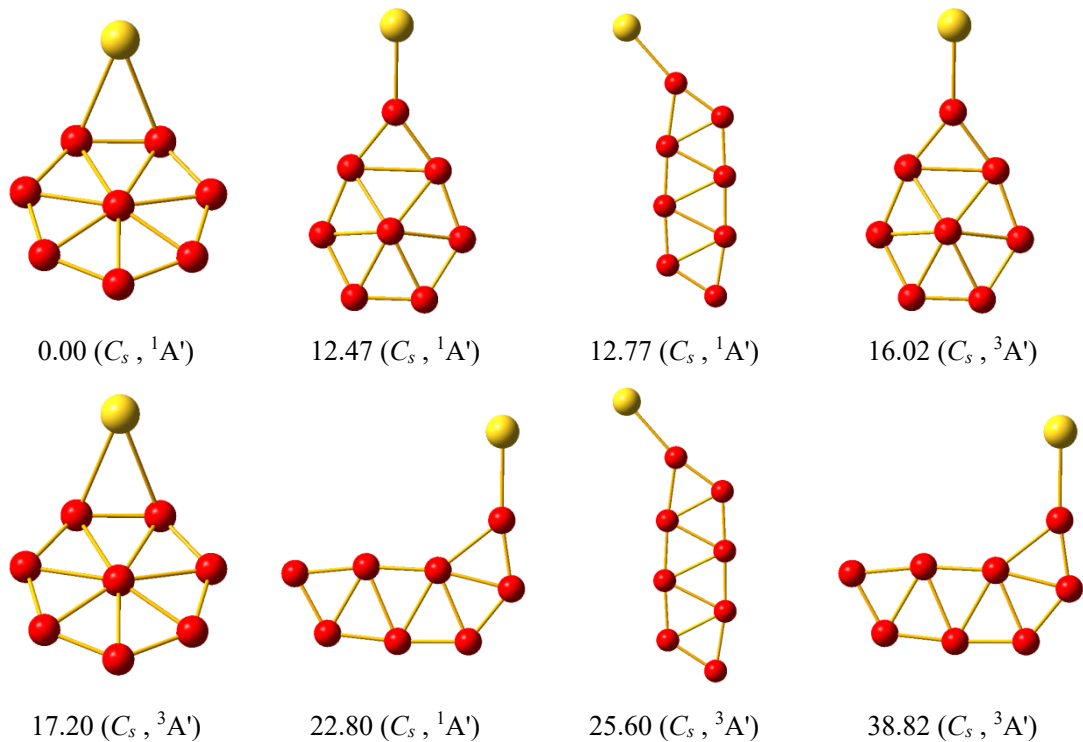


**Fig. S1** Low-lying isomers of  $AuB_8^-$  and their symmetries and electronic states at the PBE/TZP level with the SR-ZORA effect. The relative energies are given in kcal/mol. Note that the highly symmetric  $Au@B_8^-$  isomer is a much higher energy structure (>100 kcal/mol).

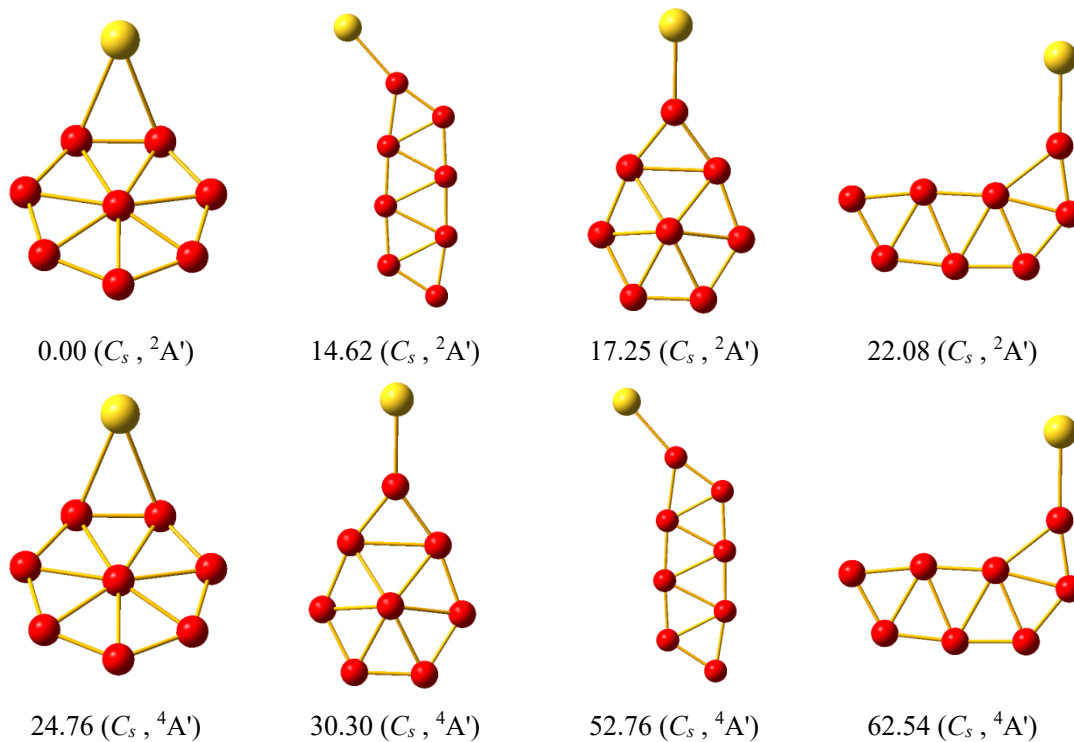


**Fig. S2** Low-lying isomers of  $AuB_8$  and their symmetries and electronic states at the PBE/TZP level with the SR-ZORA effect. The relative energies are given in kcal/mol.

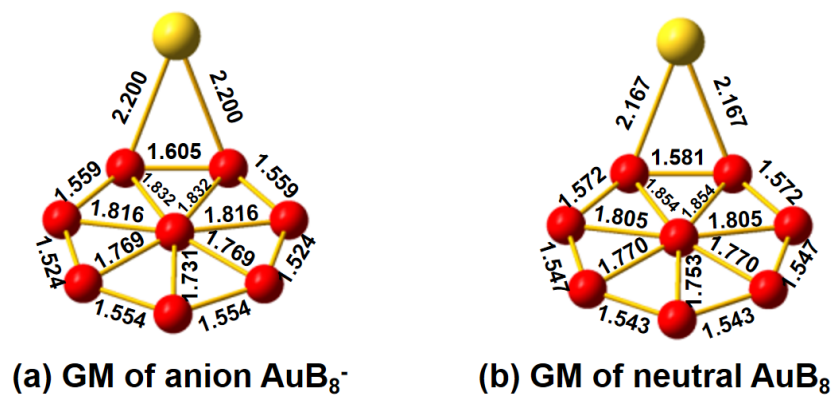


**Fig. S3** The bond lengths of the global minima of (a)  $AuB_8^-$  and (b)  $AuB_8$  optimized at the PBE0/TZP level with the SR-ZORA effect.

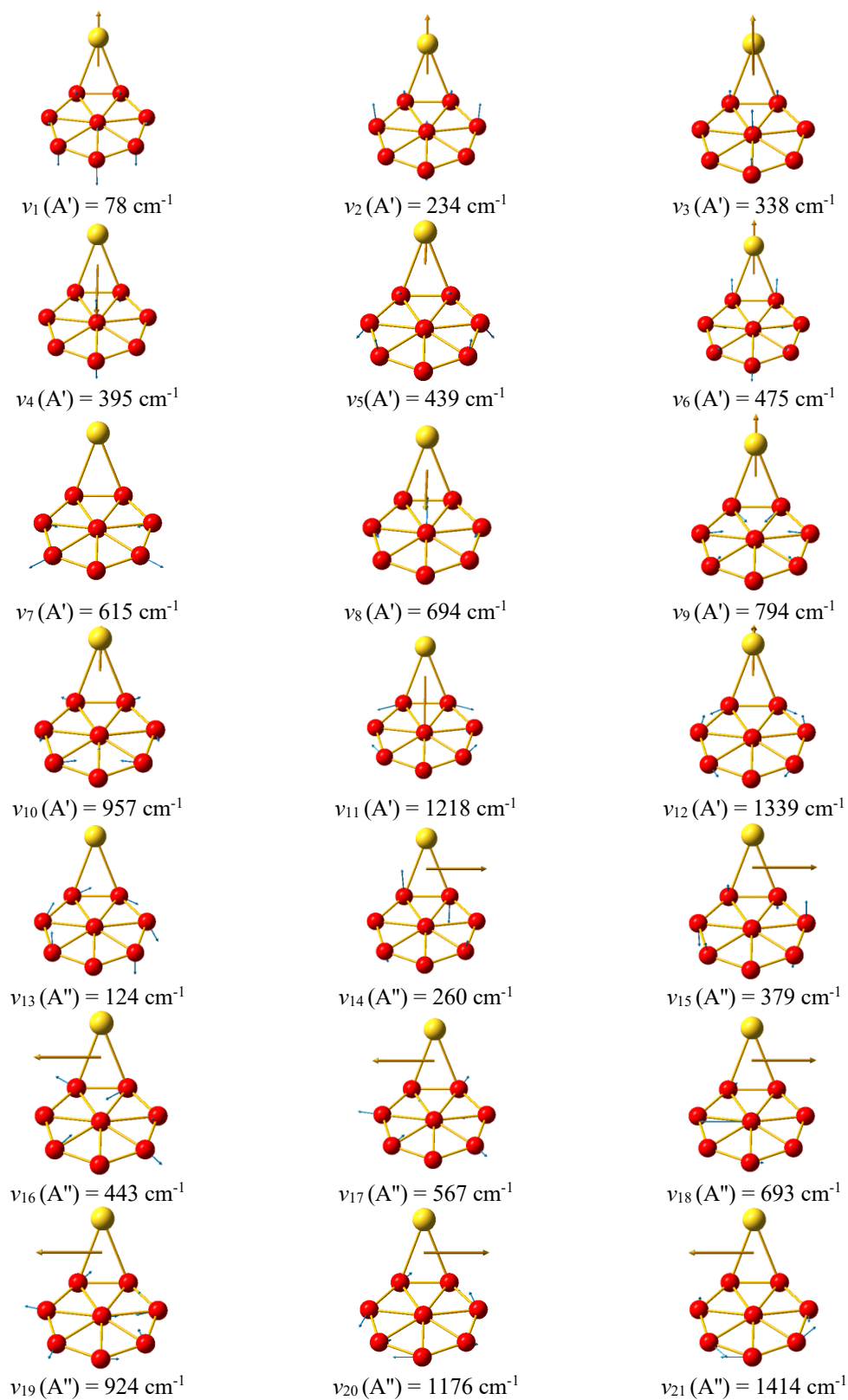


**Fig. S4** The atomic displacement vectors of the vibrational modes for the GM of  $\text{AuB}_8$  ( $C_{8s}, {}^2A'$ ). The symmetries and the calculated frequencies at the B3LYP/LANL2DZ/6-311G\* level are given.

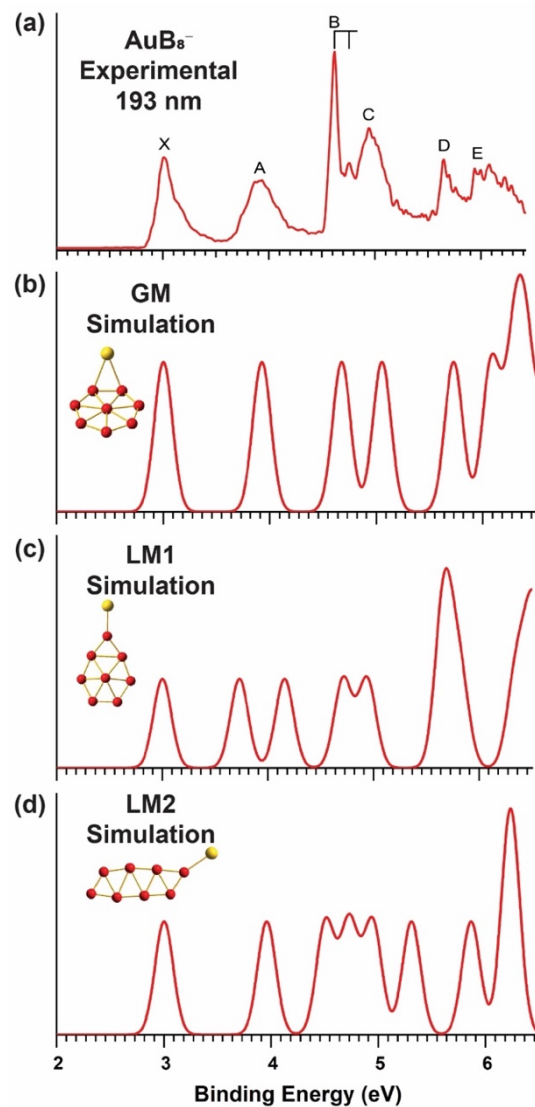
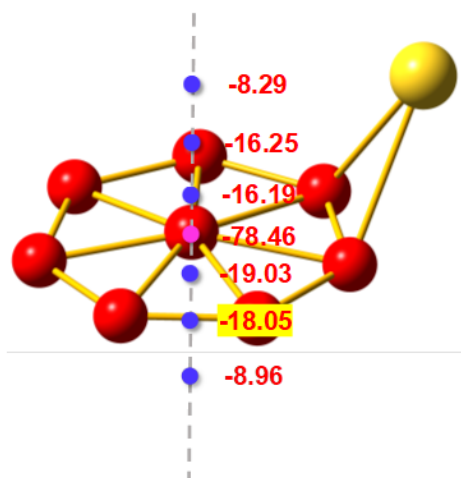
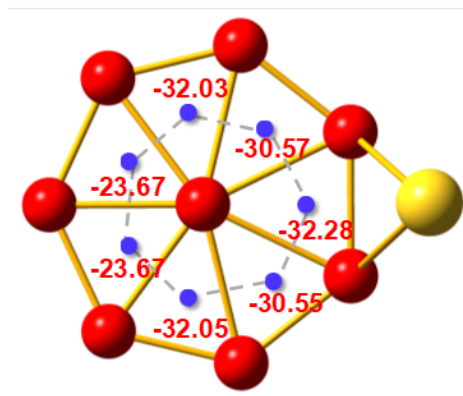


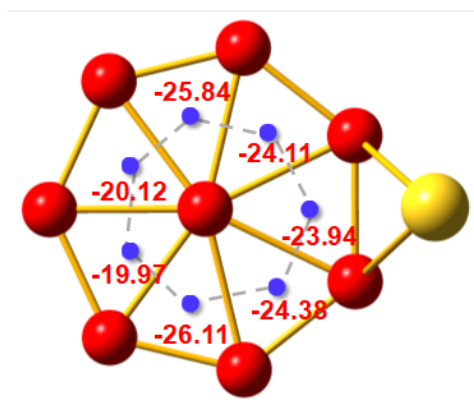
**Fig. S5** Comparison of the experimental photoelectron spectrum of  $\text{AuB}_8^-$  with the simulated spectra of the GM (b) and the two low-lying isomers (c) and (d) at the TD-SAOP/TZP level.



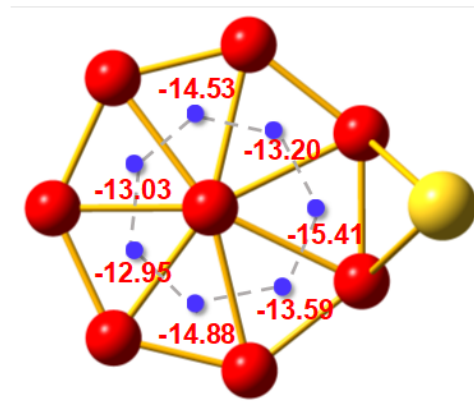
(a) Along with the z axis



(b) In the center of each B<sub>3</sub> ring



(c) 0.5 Å above the center of each B<sub>3</sub> ring



(d) 1.0 Å above the center of each B<sub>3</sub> ring

**Fig. S6** The Nucleus Independent Chemical Shifts (NICS) (in ppm) of the GM of anionic AuB<sub>8</sub><sup>-</sup> calculated at the PBE/TZP level with the SR-ZORA effect. The distance between adjacent points in (a) is 0.5 Å.



**Table S1** The experimental first ADE and VDE (in eV) of  $\text{AuB}_8^-$  in comparison with the calculated values at the PBE/TZP and PBE0/TZP level.

	ADE			VDE		
	Exp <sup>a</sup>	PBE	PBE0	Exp <sup>a</sup>	PBE	PBE0
	2.96	2.91	2.78	3.00	2.97	2.84

<sup>a</sup>The experimental uncertainty was estimated to be  $\pm 0.03$  eV.

**Table S2** The calculated atomic charges on the Au and B atoms in the GM of  $\text{AuB}_8^-$  with different partition schemes at the PBE/TZP level.

Atoms	Mulliken	Hirshfeld	Voronoi	MDC-m	NPA
Au	0.067	0.014	0.009	0.072	0.216
B	-0.209	-0.111	-0.111	-0.108	-0.059
B	-0.242	-0.157	-0.171	-0.164	-0.201
B	-0.290	-0.146	-0.160	-0.181	-0.268
B	-0.11	-0.159	-0.170	-0.167	-0.171
B	-0.290	-0.146	-0.162	-0.181	-0.268
B	-0.242	-0.157	-0.171	-0.164	-0.201
B	-0.191	-0.159	-0.170	-0.167	-0.172
B	0.586	0.022	0.106	0.061	0.123

**Table S3** The Cartesian coordinates of the GM and LM for AuB<sub>8</sub><sup>0/-</sup> optimized at the PBE0/TZP level with the SR-ZORA effect.

GM of AuB <sub>8</sub> <sup>-</sup>			
Au	0.97620250	0.00016666	0.11904837
B	-3.62922400	-0.00050043	0.66391863
B	-3.04236593	1.40696640	0.36331005
B	-0.72025612	0.80273468	-1.02958581
B	-1.76176083	-1.76504031	-0.38284829
B	-0.71985824	-0.80192990	-1.02989069
B	-3.04162411	-1.40760620	0.36311400
B	-1.76239249	1.76523831	-0.38209712
B	-2.06725578	-0.00001620	-0.08244414
LM1 of AuB <sub>8</sub> <sup>-</sup>			
Au	-1.47053877452351	-0.00161089711262	0.07207337387791
B	0.53898270246429	-0.00087572874166	0.06378847294263
B	4.67333052406012	-0.77082841994011	0.12401463205812
B	1.83135724221544	-0.89723516314950	-0.19241114019020
B	4.67268677828790	0.77242573535213	0.12414075502998
B	1.83068332849739	0.89647522216162	-0.19268636704094
B	3.32678140307457	-1.55962440912550	-0.22376174315598
B	3.32558904932670	1.56006169563099	-0.22390330942451
B	3.21006374659709	0.00019696492465	0.37244432590300
LM2 of AuB <sub>8</sub> <sup>-</sup>			
Au	1.59703035987080	0.08462978457245	-0.00024758344346
B	-5.97808318904130	0.16661864942925	0.00011962168604
B	-0.31662053925860	-0.47517126639885	-0.00018478149197
B	-4.59855665663790	-0.53657717204959	0.00008262758461
B	-1.52601932953872	-1.44871663752125	-0.00005408532198
B	-3.28871088497865	0.82183839082355	-0.00007669832173
B	-1.80626447445245	0.20853691848976	-0.00015339363523
B	-4.83461232801473	1.15541647606570	-0.00001949782046
B	-3.02202895794844	-0.99634414341102	0.00002879076418
GM of AuB <sub>8</sub>			
Au	1.03558541199033	0.00015194170269	0.05189325515996
B	-3.66904386471296	-0.00050714561089	0.65997066846953
B	-3.07992623430627	1.39245140494750	0.35617706800285
B	-0.68591473076775	0.79106557112025	-1.00101861241713
B	-1.76889891240984	-1.74795003388444	-0.38543380480764
B	-0.68565271591381	-0.79024764115653	-1.00154586269471
B	-3.07914326191918	-1.39310671344478	0.35604760449854

B	-1.76958686185611	1.74817203160895	-0.38477622080131
B	-2.06595383010441	-0.00001641528275	-0.04878909541009
LM1 of AuB <sub>8</sub>			
Au	1.51909377944692	0.22644380683070	-0.00029175470681
B	-5.99953203060385	0.23940859752382	0.00009989249346
B	-0.27300804657077	-0.58009999608823	-0.00015626427783
B	-4.56023532792070	-0.49915682434441	0.00006657862257
B	-1.51831305264091	-1.46956818025398	-0.00004248635590
B	-3.28812898047914	0.73580401426466	-0.00006607598973
B	-1.79714600840746	0.16300293464967	-0.00011519059805
B	-4.81231055439484	1.17992777792189	-0.00001487646563
B	-3.04428577842923	-1.01553113050412	0.00001517727792
LM2 of AuB <sub>8</sub>			
Au	-1.42397360977157	-0.00034412853687	0.11287694978070
B	4.57192798251697	0.77157557214272	0.29147249062613
B	1.81041949010779	-0.94391642450944	-0.39526686996239
B	0.51465507626456	-0.00053039621675	-0.28100072610349
B	3.04102997470027	0.00017431334631	0.44540382641635
B	3.29659532075466	-1.52717654613079	-0.25852914567611
B	3.29535092191989	1.52795710913442	-0.25791888963554
B	4.57239267788233	-0.77125009701542	0.29299286079349
B	1.80966016562511	0.94416059778581	-0.39485449623914